applied optics

Study on a wideband, variable aperture, high resolution scatterometer for planar diffraction grating stray light measurement

Jin Yang,[1,2,*] Rui Zhang,[1,2] Lu Yin,[1,2] Ci Sun,[1] and Tianjiao Li[1]

[1]Grating Technology Laboratory, Changchun Institute of Optics and Fine Mechanics and Physics, Chinese Academy of Sciences, Changchun, Jilin 130033, China
[2]University of Chinese Academy of Sciences, Beijing 100049, China
*Corresponding author: yang_jin1988@163.com

Received 3 October 2016; revised 27 November 2016; accepted 2 December 2016; posted 5 December 2016 (Doc. ID 277968); published 9 January 2017

Stray light is one of the important factors for evaluating the quality of gratings. Therefore, it has become an important problem in the field of grating development to measure the stray light of planar diffraction gratings accurately. For that reason, a planar grating stray light testing instrument based on a Czerny-Turner (C-T) structure has been studied. On the premise of the low stray light of the instrument itself, the instrument is capable of measuring wideband, variable aperture, and high resolution stray light for planar gratings. A scatterometer dynamic range of over nine orders has been demonstrated. Based on the scalar diffraction theory and classical Fresnel-Kirchhoff diffraction theory, the optical and mechanical model of the scatterometer is designed, which is irradiated by parallel light, and the simulation results are analyzed. The instrument realizes the measurement of the grating distribution function (GDF). And with reference to the expression form of the bidirectional reflectance distribution function (BRDF), the measurement data of the instrument is associated with the power spectral density (PSD). Through the optical integrated design and stray light suppression design, full aperture (15 mm × 15 mm–200 mm × 200 mm) and wideband (380–900 nm) measurement for any number of lines grating is realized, and the efficiency of equipment usage is improved. Experimental results show that based on the attenuation method, the accuracy of measurement can be 10^{-9} by the replacement of the neutral density filters.

OCIS codes: (050.0050) Diffraction and gratings; (120.0120) Instrumentation, measurement, and metrology; (120.4640) Optical instruments.

http://dx.doi.org/10.1364/AO.56.000247

1. INTRODUCTION

The application of spectral analysis technology in the field of scientific research, national defense construction, economic development, and people's livelihood is becoming more and more common. The grating is a key component of spectral analysis technology [1–3]. Therefore, the fabrication of high quality gratings has become one of the core of the development of high precision spectral analysis instruments. The stray light is an important index of the quality of the grating, especially the high resolution grating. Stray light is mainly caused by the defects of gratings, and it decreases the signal-to-noise ratio of the spectral instrument greatly. Stray light directly affects the measuring range and measuring precision of high precision spectrometers. Only through measuring the stray light's strength accurately can we calculate, judge, and deal with the harm brought to spectral data by stray light.

At present, the precise measurement of stray light is still difficult, and there is no uniform testing method [4–8]. Asmail and Cromer [5] and Neubert and Seifert [6] introduced a scatterometer using a convergent beam based on the bidirectional reflectance distribution function (BRDF). Weigel [7] and Loewen [8] used this type of instrument to measure the grating stray light. However, using convergent light to measure the grating used in the parallel light will have a bigger error, which will affect the final measurement accuracy. Moreover, BRDF theory, which meets the measurement conditions of Rayleigh scattering, is mainly used for measuring the stray light of a rough surface. However, the groove of the grating [9,10] is generally larger than λ, which does not meet the Rayleigh scattering conditions. The theoretical basis of the measurement is not perfect, and it is difficult to invert the defect of gratings from the measured data. Based on the scalar diffraction theory

and classical Fresnel-Kirchhoff theory, using a parallel beam to measure a high density grating has a more strict derivation [11]. The parallel light used to measure the grating distribution function (GDF) can improve the measurement accuracy. While the theory is relatively perfect, defects can be retrieved from the measured data. According to the BRDF expression, the measurement data are associated with the power spectral density (PSD). Woods and Wrigley [12] and Kuznetsov and Content [13] introduced the scatterometer based on GDF theory. Their testing instruments use the Littrow structure to measure the stray light of the grating under the condition of parallel light. However, since the Littrow structure is relatively compact, it is difficult to eliminate the stray light inside the instrument. Also, the spherical mirror in the back end that acts as both the collimating mirror and the focusing mirror causes secondary stray light, which makes the requirements of the spherical mirror surface's accuracy higher. Based on the GDF theory, a scatterometer for the planar diffraction grating is designed using a Czerny-Turner (C-T) structure in this paper. In the instrument, a zoom and beam expander system is designed which can carry out full aperture measurement of different aperture gratings. The dispersion subtraction double monochromator structure provides monochromatic light, the spectral resolution of which is above 0.2 nm, in the whole wavelength range. Meanwhile, it can suppress the stray light and remove the interference light in the source. The neutral density filter can be replaced at any time in the energy control system, which can increase the dynamic measuring range of the instrument. The grating of different line number and full aperture (15 mm × 15 mm–200 mm × 200 mm) at the wavelengths ranging from 380 to 900 nm can be measured by the instrument, and the accuracy of measurement can be 10^{-9}.

2. THEORY OF THE SCATTEROMETER FOR THE DIFFRACTION GRATING

The stray light of the diffraction grating is mainly caused by the Fraunhofer diffraction and the defects of the grating itself. Under the condition of parallel light incidence, based on the classical Fresnel-Kirchhoff and scalar diffraction theories, combined with the statistics theory, the expression of stray light intensity in the instruments can be written as [13]

$$R(\lambda_t,\lambda_o)=\frac{\Delta\lambda}{N\lambda_o}\cdot\frac{\sin c^2\pi\left(\frac{\lambda_t-\lambda_B}{\lambda_o}\right)}{\sin c^2\pi\left(1-\frac{\lambda_B}{\lambda_o}\right)}\cdot\frac{1}{1-\cos\left(2\pi\frac{\lambda_t}{\lambda_o}\right)}\cdot\left\{1+\left[1+Nb\left(2\pi\frac{\lambda_t}{\lambda_o}\right)^2\right]\right\}\cdot+\frac{\pi^2\Delta\lambda}{\lambda_o^3}\cdot\left(4-\frac{\lambda_t^2}{d^2}\right)^2\cdot\frac{1}{\sin c^2\pi\left(1-\frac{\lambda_B}{\lambda_o}\right)}\cdot\left[\sigma_d^2\cdot\sin c^2\pi\left(\frac{\lambda_t-\lambda_B}{\lambda_o}\right)+\frac{q\pi\alpha^2\sigma_r^2}{df\lambda_o}\right],\quad(1)$$

$$\Delta\lambda=\frac{W}{nf}\cos\beta.\quad(2)$$

$\Delta\lambda$ is the output bandwidth of the instrument, W is the width of the slit before the detector, n is the grating constant, f is the focal length of the focusing lens of the measurement system, β is the diffraction angle, N is the total number of grating lines, λ_o is the central wavelength of the monochromatic light, λ_t is the wavelength of stray light within the scope of the study, and λ_B is the blazed wavelength. $B=\sigma 2/2d$, σ is the standard deviation of groove spacing of the grating, σ_d is the standard deviation of groove depth of the grating, q is the height of the exit slit, α is the autocorrelation function of the surface roughness of the grating, and σ_r is the position deviation of grating surface defects. The formula reflects the inherent stray light of the grating, the stray light which is introduced by the random error of the grating groove interval, the stray light which is introduced by the random error of the grating groove depth, and the stray light which is introduced by random defects on the surface of the grating.

Under the condition of parallel light illumination, the GDF is measured by the attenuation method, which measures the stray light near the main spectrum wavelength by rotating the grating. Combined with the formula (1), the stray light measurement result is described by relative intensity:

$$\mathrm{GDF}(\lambda_t)=\frac{I_m(\lambda_t)-I_d}{I_o-I_d}\cdot\frac{T(\lambda_t)}{T_o}\cdot\frac{\Delta\lambda_o}{\Delta\lambda(\lambda_t)},\quad(3)$$

where I_m is the current of stray light received by the detector in different wavelength displacements, I_o is the current of the main spectrum, I_d is the detector dark current, and T is the coefficient of light intensity attenuation. GDF(λ) is a series of values which is related to the wavelength displacement. By measuring the displacement of the main spectral line with different wavelengths, the curve of GDF(λ) – λ can be obtained, which can quantitatively evaluate the stray light level of the diffraction grating.

Making reference to the BRDF expression [6,7,14], the measurement data are associated with the PSD, and the other expression of GDF can be written as

$$\mathrm{GDF}(\theta_s)=\frac{I_m(\theta_s)-I_d}{I_o-I_d}\cdot\frac{T(\theta_s)}{T_o}\cdot\frac{d\Omega}{\cos\theta_s}=4\left(\frac{2\pi}{\lambda}\right)^4\cdot\cos\theta_i\cdot\cos\theta_s\cdot Q\cdot\mathrm{PSD}(f),\quad(4)$$

where $d\Omega$ is the solid angle of the detector, θ_s is the scattering angle, θ_i is the incident angle, Q is a factor which is related to the instrument and the surface measured, and PSD(f) is the PSD of space frequency. Through PSD, the measurement results of the instrument, the measurable surface parameters of the grating, and the simulation results can be combined. All of the surface parameters of the grating can be calculated.

3. DESIGN OF THE INSTRUMENT

A. Brief Introduction of the Instrument

The schematic diagram of a planar diffraction grating scatterometer is shown in Fig. 1. The instrument is mainly composed of seven parts: the light source and energy monitoring system, the zoom and beam expander system, the double monochromatic system, the energy control system, the measuring system, the receiving system, and the control system.

The instrument was made in a class 10,000 clean room since a dust-free environment is critical for obtaining stray light data

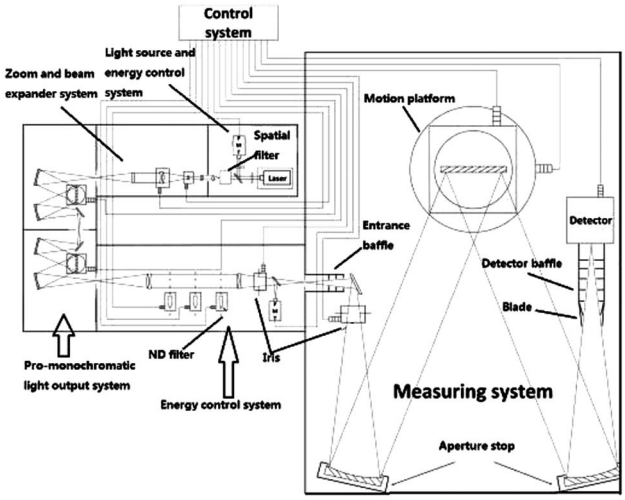

Fig. 1. Schematic diagram of scatterometer.

over nine orders of dynamic range. The modules of the instrument are connected functionally and placed on the optical platform, which can change the modules flexibly and is easy to install and reconcile. At present, a 632.8 nm laser is used as the light source. A Nikon 10 × objective and Newport 5 μm pinhole are adopted to form the spatial filter. Behind the pinhole a commercial lens collimates the light before it enters the back-end system. Considering the experimental properties and the extended application of the instrument, the wavelength range of the back-end system is 380–900 nm, and the light source system can be replaced by a continuous light source module. The energy attenuation of three orders can be reached through the replacement of neutral density filters, and the dynamic range of six orders can be reached through the measuring system. The accuracy of measurement can be 10^{-9}.

B. Design of the Optical System

A scatterometer for planar diffraction gratings is similar to a spectrometer. For a general spectrometer, usually the aberration at the direction of dispersion is focused on, in order to ensure the high spectral resolution, but the aberration has great influence on the stray light of the instrument itself. There are several slits and pinholes installed on the focus of the intermediate imaging plane in the scatterometer. Coma and astigmatism can make the focus diffuse. There is scattering at the edge of slits and pinholes, which can increase the stray light of the instrument itself. Therefore, the difference of optical design between the scatterometer and the general spectrometer system is that the astigmatism and coma at the direction of vertical dispersion have more stringent requirements. At the same time, the suppression of the stray light of the instrument itself should be taken into consideration.

1. Zoom and Beam Expander System

System modules are connected by a variable slit. According to the formula $W = 1.22\lambda F\#$, laser focus size changes at different F#. The zoom and beam expander system is used to make most of the energy at different F# pass into the slit. With the iris, the laser spot diameter is adjustable from 0.75 to 2 mm. The laser

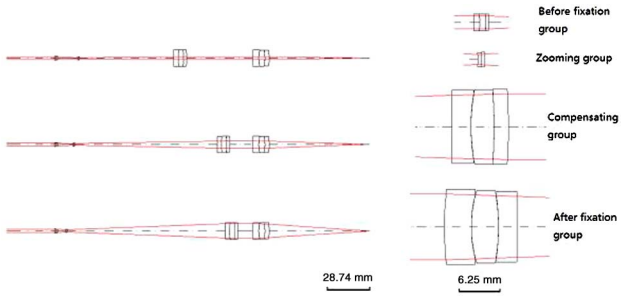

Fig. 2. Optical layout of zoom and beam expander system.

light enters the space filter and is collimated. With the four sets of zoom systems, F# can realize a continuous change from 0.005 to 0.067. In the measurement system of 1.5 m focal length, the measurement of the grating of 15 mm × 15 mm – 200 mm × 200 mm is completed. A combination of achromatic lenses is used in the system. Chromatic and spherical aberration are corrected, respectively, and the residual aberration and apochromatism are corrected by the combined lens, which can realize the measurement at wavelengths ranging from 380 to 900 nm. As shown in Fig. 2–5, the optical modulation transfer function (MTF) of the system is close to the diffraction limit, and imaging quality is high.

2. Double Monochromatic System

The double monochromatic system using a dispersion subtraction double monochromator structure provides monochromatic light with the spectral resolution above 0.2 nm and can suppress the stray light and remove the interference light in the source. The symmetric C-T structure and dispersion subtraction structure suppress the off-axis aberration, and the off-axis parabolic mirror corrects spherical aberration and astigmatism, which reduces the stray light inside the instrument and ensures the energy in the instrument. Figure 6 shows the optical structure of the double monochromatic system. Figure 7 shows the aberration curves at different wavelength bands. Figure 8 shows the spot diagram at the resolution of 0.2 nm.

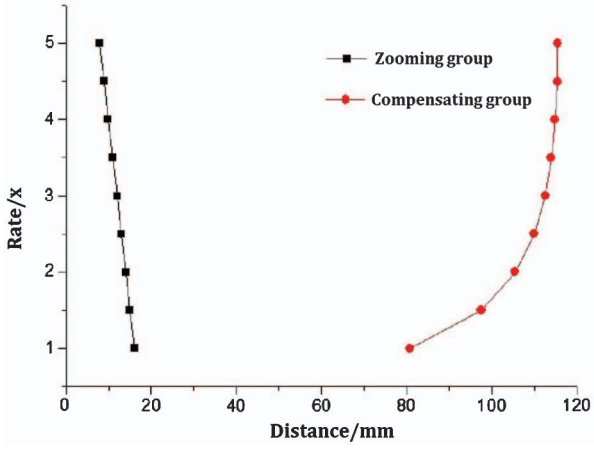

Fig. 3. Cam curve of zoom and beam expander system.

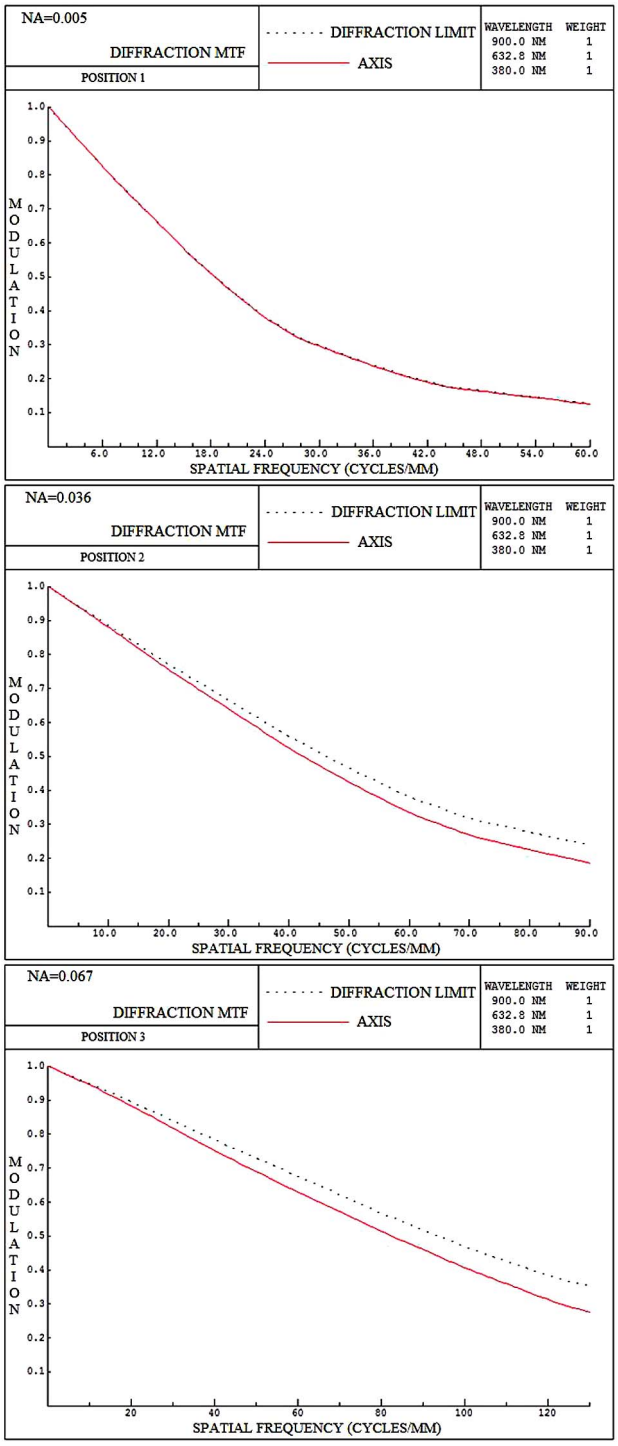

Fig. 4. MTF of zoom and beam expander system.

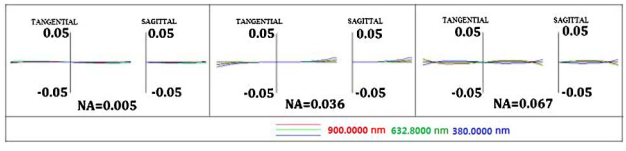

Fig. 5. Aberration curve of zoom and beam expander system.

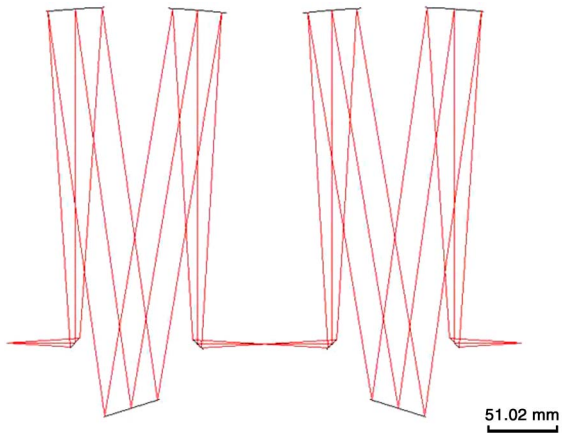

Fig. 6. Optical layout of double monochromatic system.

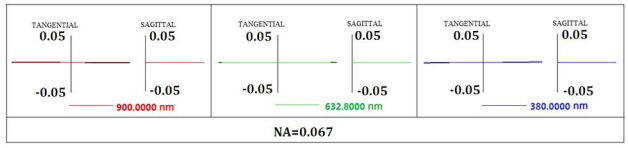

Fig. 7. Aberration curves at different wavelength bands.

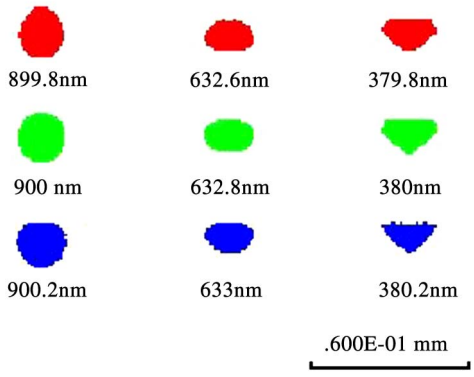

Fig. 8. Spot diagram at the resolution of 0.2 nm.

3. Energy Control System

The energy control system is used to adjust the energy of the light into the measurement system with high precision by inserting a certain number of neutral density filters into the light path and providing a parallel beam on the premise of making no change to the system's numerical aperture. In addition, in order to reduce the stray light of the instrument itself, the mirror in the measurement system should have high quality surface precision and specular roughness. As parabolic mirrors, which are difficult to process, cannot be used in the measurement system, the energy control system needs to provide some residual spherical aberration to correct the spherical aberration of the measurement system. The numerical aperture matching is completed by using a fully symmetrical structure. An achromatic lens system is used to correct chromatic aberration.

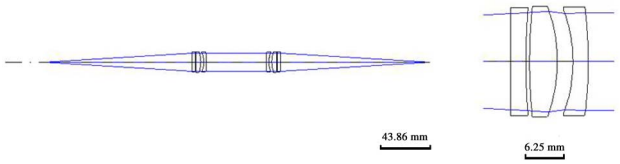

Fig. 9. Optical layout of energy control system.

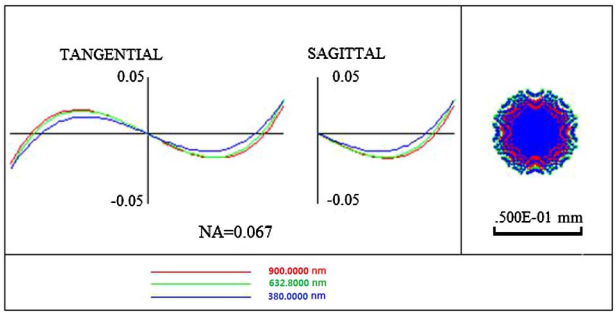

Fig. 10. Aberration curve and spot diagram.

Figure 9 shows the optical structure of the energy control system, and Fig. 10 shows the aberration curve and the spot diagram.

4. Measuring System

The measurement system is actually a monochromator system. Strict chromatic aberration correction and consistency of the full wave aberration are needed for the system. The asymmetric C-T structure with total reflection is used to correct coma. A cylindrical mirror is used to correct astigmatism. As the stray light level of the instrument is inversely proportional to the focal length, in order to reduce the stray light of the instrument, the reflection system uses a long focal length mirror which is 1.5 m. At the same time, spherical mirrors, which can easily realize the super smooth and high surface accuracy, are used. Figure 11 shows the optical structure of the measuring system, and Fig. 12 shows the aberration curve of each wave band.

5. Integrated Optical System

According to the modular design, each module is a relatively independent system. When all the modules are combined,

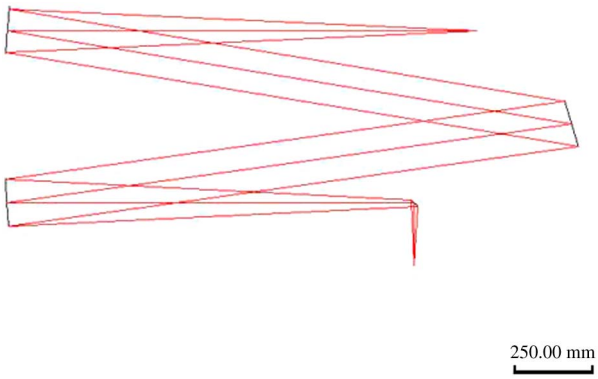

Fig. 11. Optical layout of the measuring system.

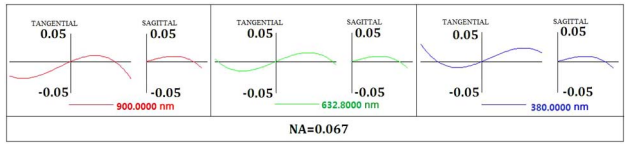

Fig. 12. Aberration curve of each wave band.

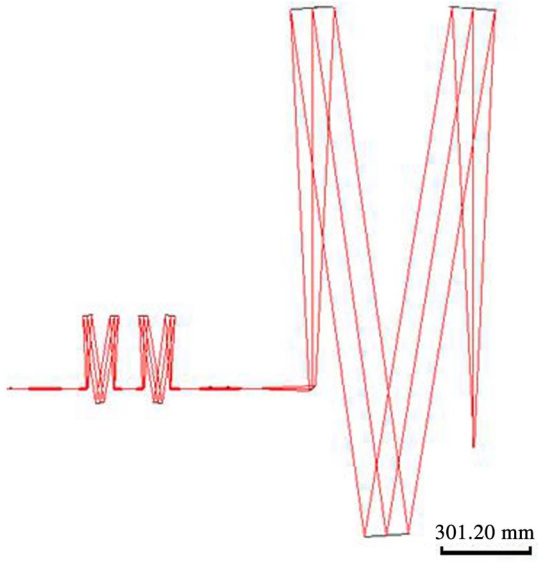

Fig. 13. Optical layout of the whole system.

the problem of the aberration superposition and the system matching comes up. Each subsystem of the instrument has a certain degree of complexity. This inevitably leads to a decline in imaging quality when the subsystems are integrated. However, the instrument has higher requirements for the energy and the stray light. Therefore, the whole system uses an integrated optimization design; that is, the design of the subsystems is based on strict system matching. Under the premise of the realization of their own functions, the subsystems should also take aberration cancellation into consideration. The optical structure of the whole system is shown in Fig. 13. Figure 14 shows the analysis results of different grating grooves. It is shown that the aberrations of the whole system at different wavelengths are suppressed successfully and the image quality is uniform.

C. Stray Light Suppression of the Instrument

The scatterometer is used to measure the stray light of gratings, which requires the stray light level of the instrument to be lower than that of the grating to be measured, so that the direct measurement of the grating's stray light can be realized. For the whole system, because of the front double monochromator, the matched aperture stops, the entrance slit, and the entrance baffle, the outside stray light into the measurement system is almost negligible. Therefore, the suppression of the instrument's stray light is mainly the internal stray light suppression of the measurement system.

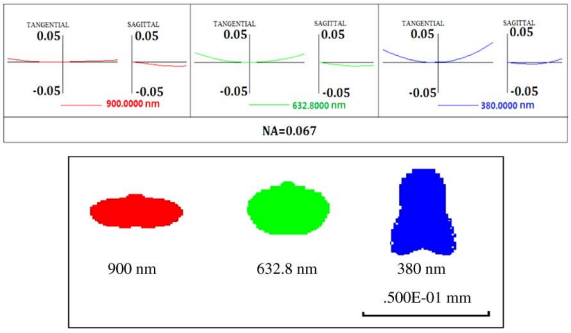

(a)

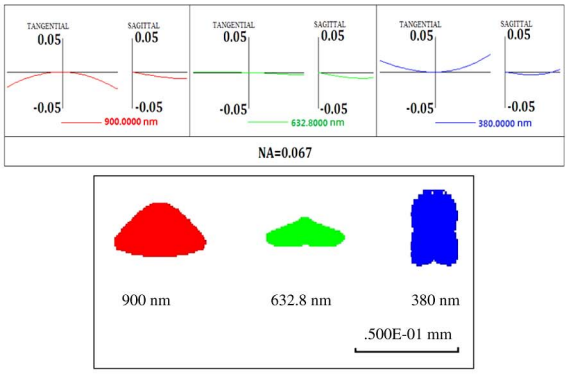

(b)

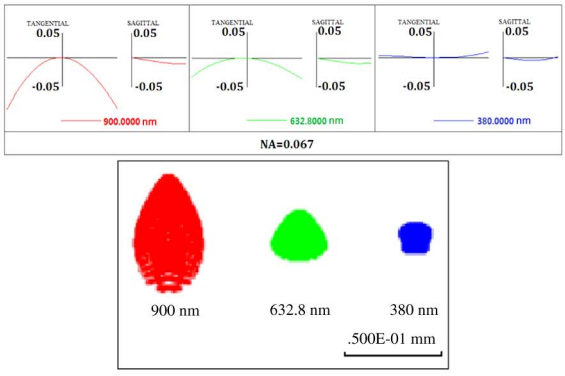

(c)

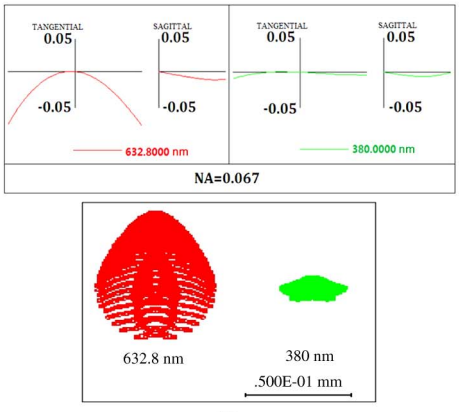

(d)

Fig. 14. Analysis results of different grating grooves. (a) Aberration curve and spot diagram of 300 gr/mm. (b) Aberration curve and spot diagram of 600 gr/mm. (c) Aberration curve and spot diagram of 1200 gr/mm. (d) Aberration curve and spot diagram of 1800 gr/mm.

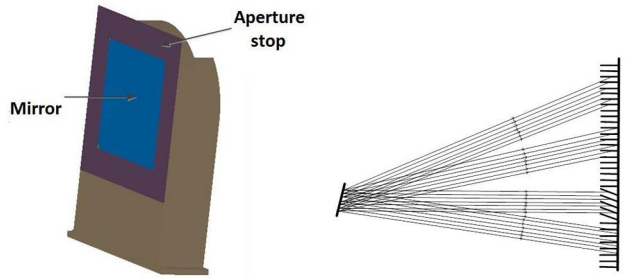

(a) (b)

Fig. 15. Structure of aperture stop and light trap. (a) Aperture stop. (b) Light trap.

The main sources of the instruments' stray light are multiple diffraction of the grating and light scattered off the walls and stents. First of all, to reduce the unwanted reflections, aperture stops are added in front of all mirrors matched with the system's numerical aperture, as is shown in Fig. 15(a). So only the main optical path of light can reach the mirrors, which can effectively suppress multiple diffraction of the grating. Second, the light traps are added at the important area on which grating diffraction light directly irradiates, as is shown in Fig. 15(b). As the diffraction light is scattered multiply in the light trap, the stray light's paths back to grating and its intensity are reduced. At the same time, the scattering of the inner walls is suppressed. In addition, the inner walls and stents are brushed with a black paint made for the special purpose of light extinction. The special material and the processing technology are adopted to reduce the stray light generated by the entrance slit. As the stray light of the instrument is inversely proportional to the focal length, a long focal length reflection system is used, and the focal length of the mirror is 1.5 m. Another component path of the stray light of the instrument itself is the scattering from optical elements. In consideration of the difficulty of supersmooth surface processing, the system adopts a spherical mirror as the collimating mirror and converging mirror; the mirror should have high quality surface precision, the RMS of which is less than $\lambda/40$, and the roughness of the surface and the film should be less than 0.6 nm to reduce the stray light generated by the mirror. Finally, the baffle and blades are added in front of the detector as shown in Fig. 16. Through a series of extinction

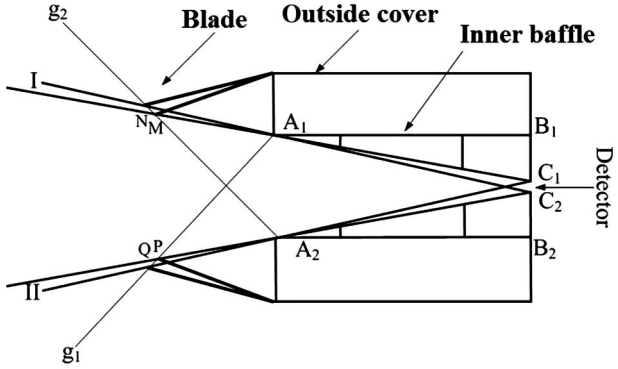

Fig. 16. Structure of baffle.

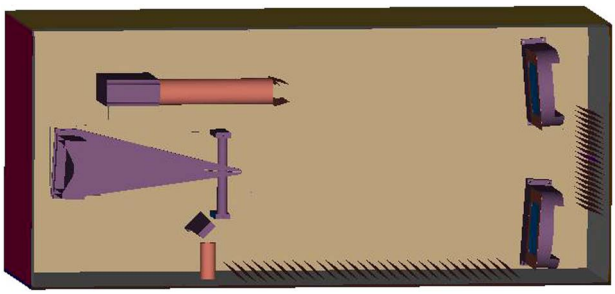

Fig. 17. System structure model.

treatments to reduce the level of the stray light of instrument, the system structure model is shown in Fig. 17.

The structure model of the instrument is further improved by using the simulation software to calculate and analyze the system's stray light. First, we need to specify the scattering model of each component surface. Whether the parameters of the model are reasonable or not is an important factor to affect the accuracy of the simulation results. The inner walls and stents again are coated with high absorbing material, the absorbing coefficient of which is 0.905, and the scattering model is Lambertian. The mirror is a Harvey model, and the surface roughness of P is <1 nm, while the reflectivity of $R = 0.985$. Second, the parameters of the diffraction grating such as the energy distribution are calculated by simulation software at common grating grooves of 300, 600, and 1200 gr/mm. Finally, the simulation results of the completed system structure model are shown in Fig. 18. The maximum stray light of the three kinds of grating mentioned is 1.75×10^{-9}, 7.05×10^{-10}, and 2.75×10^{-13}, respectively. The average value of stray light is 1.29×10^{-10}, 6.32×10^{-11}, and 2.99×10^{-14}. The more grating grooves there are, the less stray light.

The mechanical design and processing of the instrument are based on the optical design and stray light simulation results. The top of the aperture stops and the blades are wedge-shaped, black-anodized, and polished to reduce the edge scattering and diffraction of surface. The motion platform control test angle is in the ±30 deg range, and the angular resolution less than 0.6 arcsec. In actual processing, the absorption rate and the

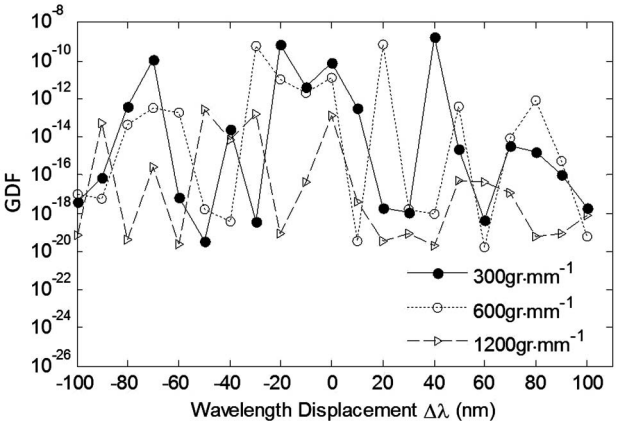

Fig. 18. Relative intensity of grating stray light at different grooves after the stray light suppression.

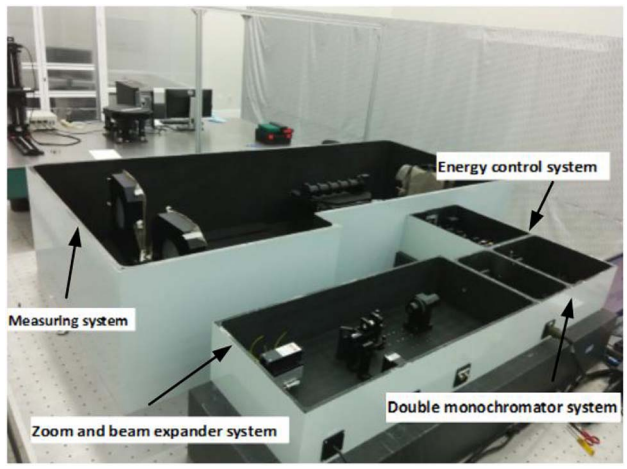

Fig. 19. Physical layout of the instrument.

roughness of the optical elements are higher than those shown in the simulation results. The elimination of the stray light calibration of the instrument can meet the requirements of the measurement, and the final physical layout is shown in Fig. 19.

4. MEASUREMENT RESULTS AND ANALYSIS

The instrument achieves precise scanning of the grating stray light displacement through the sine mechanism; the number

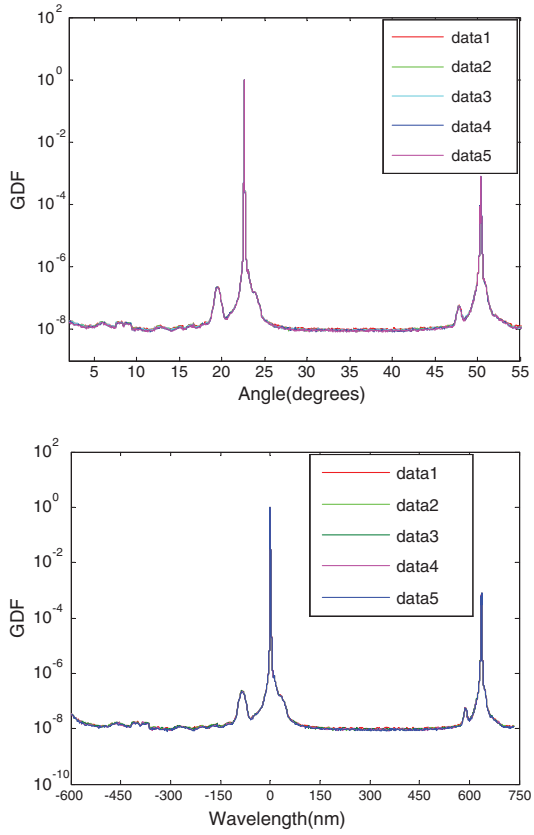

Fig. 20. Test results of 1200 gr/mm.

of steps and the angle of the stepper motor have the following relations:

$$\theta_s = \eta_0 - \arcsin\frac{s_0 \cdot g/s_c + L \cdot \sin\eta_0 - s \cdot g/s_c}{L} + c. \quad (5)$$

η_0 is the angle between the sine bar and screw when the grating is rotated to zero order light, S_0 is the number of scanning steps when the grating is rotated to zero order light, g is the pitch of the screw, S_c is the number of scanning steps when the motor is rotated in a complete circle, L is the length of the sine bar, and c is the correction constant of setup error and test samples' installation error.

According to the grating equation, the scanning equation of the C-T structure can be deduced:

$$\lambda = \frac{2\sin\theta \cdot \cos\phi_0}{n}, \quad (6)$$

where θ is the rotation angle of the grating, Φ_0 is the fixed angle in the C-T structure, and n is the number of lines of the measured grating. Thus, the relationship between the step number and the wavelength displacement of the scanning motor can be introduced:

$$\lambda_t = \frac{2\sin\left(\eta_0 - \arcsin\frac{s_0 \cdot g/s_c + L\cdot\sin\eta_0 - s\cdot g/s_c}{L} + c\right)\cdot\cos\phi_0}{n} - \lambda_o, \quad (7)$$

where λ_0 is the wavelength of incident light.

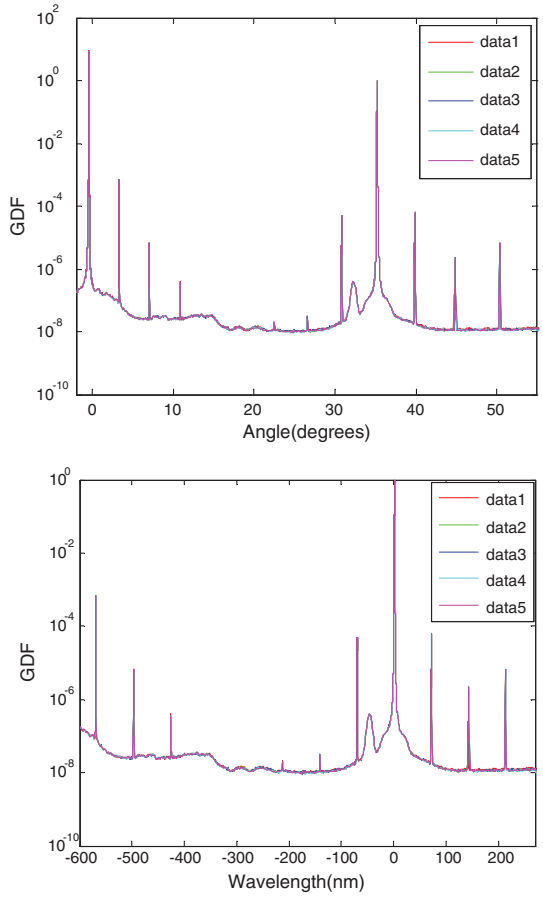

Fig. 21. Test results of 1800 gr/mm.

With the formulas (4) and (5), (3) and (7), the normalization curve of $\mathrm{GDF}(\theta_s) - \theta_s$ and $\mathrm{GDF}(\lambda_t) - \lambda_t$ of the main spectrum can be obtained. The 1200 and 1800 gr/mm ruled gratings, which are manufactured using the big ruling engine [15–17], are tested by the scatterometer. In the manufacturing process of the 1200 gr/mm grating, the ghost image and random errors are controlled in the spacing of grating grooves, but the 1800 gr/mm grating manufacture is an open-loop control. The test results are shown in Figs. 20 and 21; it can clearly be seen that the stray light and ghost image of 1200 gr/mm gratings are suppressed successfully. The repeatability of the instrument is high, and the accuracy of the measurement can reach 10^{-9}.

5. CONCLUSION

In this paper, a scatterometer for the planar diffraction grating is developed based on the scalar diffraction theory and the classical Fresnel-Kirchhoff diffraction theory, which can realize the GDF measurement of the planar diffraction grating. The instrument can be used for the full aperture (15 mm × 15 mm–200 mm × 200 mm) and wideband (380–900 nm) measurement for gratings of any number of lines. By the integrated optical design and stray light modeling, the instrument has low stray light which meets the requirements, and the measurement range can be 10^{-9}. According to formula (1), the test data can be retrieved by the least square method, and the parameters of the grating surface can be obtained. The big grating ruling engine can control the random errors in the spacing and depth of grating grooves. Through the atomic force tester we can measure the random errors. The grating's surface roughness is tested by the optical profiler. Under the condition that part of the surface parameters of the measured grating are known, the test results and simulation results are combined to improve the surface parameter inversion formula. However, the measurement range of the atomic force tester and Wyko optical profiler is only tens of micrometers. Though the overall surface is uniformly sampled, the measurement results still have deviations, and the instruments need to introduce a correction coefficient to modify its own the stray light error and alignment error. Further theoretical analysis and parameter error correction are in progress; more rigorous testing and simulation results will be reported in a subsequent article.

Funding. Chinese Finance Ministry for the National R&D Projects for Key Scientific Instruments (ZDYZ2008-1); National Natural Science Foundation of China (NSFC) (61505204); Ministry of National Science and Technology for National Key Basic Research Program of China (2014CB049500); National Key Scientific Instrument and Equipment Development projects in China (2014YQ120351).

REFERENCES

1. S. V. Bykov, B. Sharma, and S. A. Asher, "High-throughput, high-resolution echelle deep-UV Raman spectrometer," Appl. Spectrosc. **67**, 873–883 (2013).
2. C. Vannahme, M. Dufva, and A. Kristensen, "High frame rate multiresonance imaging refractometry with distributed feedback dye lasersensor," Light: Sci. Appl. **4**, e269 (2015).

3. G. Belusic, M. Llic, A. Meglic, and P. Pirih, "A fast multispectral light synthesiser based on LEDs and a diffraction grating," Sci. Rep. **6**, 32012 (2016).
4. R. E. Poulson, "Test method in spectrophotometry: stray-light determination," Appl. Opt. **3**, 99–104 (1964).
5. C. C. Asmail and C. L. Cromer, "Instrumentation at the National Institute of Standards and Technology for bidirectional reflectance distribution function (BRDF) measurements," Proc. SPIE **2260**, 52–61 (1994).
6. J. Neubert and T. Seifert, "Fully automated angle resolved scatterometer," Proc. SPIE **2210**, 543–552 (1994).
7. T. Weigel, "Stray light test methods for space optical components," Proc. SPIE **2210**, 691–699 (1994).
8. E. Loewen, *Diffraction Grating Handbook*, 6th ed. (Newport Corporation, 2005), pp. 183–188.
9. M. J. Sholl and F. S. Grochocki, "Stray light design and analysis of the SNAP telescope," Proc. SPIE **6675**, 66750C (2013).
10. J. C. Stover, "Measurement and analysis of scatter from rough surfaces," Proc. SPIE **2260**, 40–49 (1994).
11. M. R. Sharpe and D. Irish, "Stray light in diffraction grating monochromators," Opt. Acta **25**, 861–893 (1978).
12. T. N. Woods and R. T. Wrigley, "Scattered-light properties of diffraction gratings," Appl. Opt. **33**, 4273–4285 (1994).
13. I. G. Kuznetsov and D. A. Content, "Design, performance and reliability of a high angular resolution, wide angular range, large aperture fully automated UV scatterometer," Proc. SPIE **4485**, 417–428 (2002).
14. Z. Zhenrong, Z. Jing, and G. Peifu, "Roughness characterization of well-polished surfaces by measurements of light scattering distribution," Opt. Appl. **40**, 811–818 (2010).
15. L. Xiaotian and Y. Haili, "300 mm ruling engine producing gratings and echelles under interferometric control in China," Appl. Opt. **54**, 1819–1826 (2015).
16. Y. Chao and Y. Haili, "Real-time monitoring of ruling grating resolution by digital wavefront," Appl. Opt. **54**, 492–497 (2015).
17. Y. Chao and L. Xiaotian, "Practical method study on correcting yaw error of 500 mm grating blank carriage in real time," Appl. Opt. **54**, 4084–4088 (2015).